

Estimation of AUV dynamics for sensor fusion

Kjell Magne Fauske
University Graduate Center
Kjeller, Norway
Email: fauske@unik.no

Fredrik Gustafsson
Department of Electrical Engineering
Linköping University
Linköping, Sweden Email: fredrik@isy.liu.se

Øyvind Hegrenæs
University Graduate Center
Kjeller, Norway
Email: hegrenas@unik.no

Abstract—This contribution presents a method to identify dynamic models of Autonomous Underwater Vehicles (AUV) from logged data and a physically motivated model structure. Such models are instrumental for model-based control system design, but also for integrated navigation systems. We motivate our work from the perspective of developing second generation integrated navigation systems, which use a sensor fusion approach to merge external information with a dynamic model for purposes of redundancy, integrity, and for fault detection and isolation.

Keywords: AUV, Kalman filtering, estimation.

I. INTRODUCTION

Navigation of AUV's using solely inertial sensors is not sufficient, because of the inherent drift of dead-reckoning velocities and acceleration. Support in the form of sensor fusion from earth-fixed reference points is needed to avoid this drift. Information of this kind includes getting GPS fixes at the surface, acoustic baseline positioning using transponders, and bottom navigation [1].

An aided inertial navigation system (AINS) consists basically of an error state Kalman filter that estimates the drift parameters in the inertial sensors, using the external information as the measurement vector. Though AINS' are used in various applications as aircraft, autonomous vehicles in the air and at ground, in surface ships and AUV's, these AINS usually do not take the knowledge of steering commands and dynamics of the platform into account. For purely navigation purposes, knowledge of the platform dynamics is not necessary. However, a dynamic model is of interest for achieving redundancy, and for fault detection and isolation purposes. Our goal is to investigate this, and as a crucial step, we present here results on model estimation based on experimental data.

A full dynamic model of a AUV has six degrees of freedom for position and orientation, and would require 12 states to also include all linear and angular velocities. It is well known [2], that speed, steering and diving dynamics are almost decoupled for normal operation. This fact is used in control design [3]. The steering dynamics is the most crucial part, since depth is measured quite accurately and speed is mostly constant in normal operation.

This paper is organized as follows. Section II gives an overview of the HUGIN family of AUV and the current navigation system. Section III and IV describes the kinematic and dynamic equations, with an emphasis on the horizontal dynamics. Section V outlines an identification procedure for identifying parameters of the simplified model structure. The



Figure 1. The HUGIN 4500 autonomous underwater vehicle photographed during deployment.

experimental evaluation of the proposed procedure is reported in Section V.

II. SYSTEM OVERVIEW

A. The HUGIN AUV

The HUGIN 4500 AUV is the latest additions to the HUGIN AUV family manufactured by Kongsberg Maritime. The vehicle has a length of 6.5 meters and a nominal dry mass of approximately 1950 kg. Designed for large depths and long endurance, the vehicle can operate at depths down to 4500 meters and operate for 60-70 hours. The nominal cruising speed of the vehicle is about 3.7 knots or 1.9 m/s. The vehicle is passively stable in roll and close to neutrally buoyant.

B. Control inputs

For propulsion HUGIN 4500 is fitted with a large three-bladed propeller. A cruciform tail configuration with four identical control surfaces is used for manoeuvring. See Fig. 2.

C. Inertial navigation

The HUGIN 4500 vehicle is equipped with an inertial navigation system which calculates position, velocity and attitude using high frequency data from an inertial measurement unit (IMU). To counter position error growth, an error state Kalman filter is implemented which utilizes a wide range of aiding

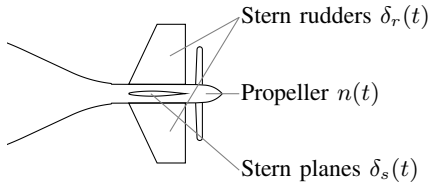


Figure 2. AUV control inputs for a cruciform tail configuration

sensor [4]. A overview of the aided navigation system is shown in Fig. 3.

Of great importance for slowing the position error growth, is the doppler velocity log (DVL), which measures with high accuracy the linear velocities of the vehicle relative to the seabed. For long submerged operations, position aiding is necessary. During survey missions the vehicle is usually tracked by a mother ship using ultra short baseline positioning (USBL) (also known as super short baseline positioning (SSBL)). Position updates are then transmitted regularly to the vehicle using an acoustic communication link.

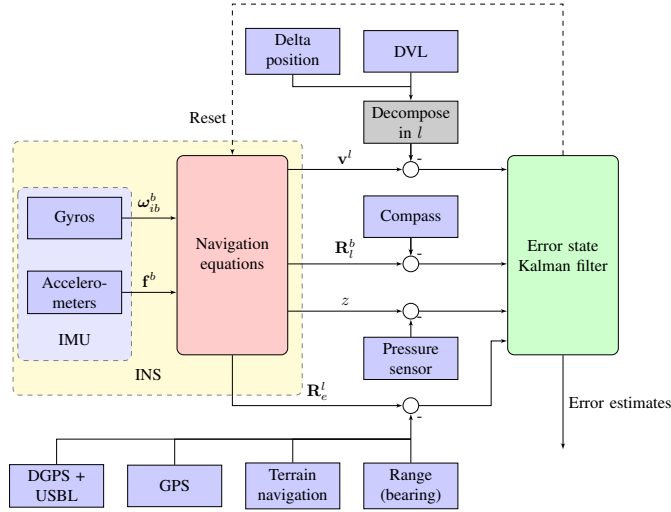


Figure 3. Aided inertial navigation system

III. UNDERWATER VEHICLE KINEMATICS

Six independent coordinates is required to completely describe the position and orientation of an underwater vehicle. For marine vehicles it is common to use the SNAME [5] notation summarized in Table I.

The coordinates are grouped into two vectors, where

$$\boldsymbol{\eta} = [x \ y \ z \ \phi \ \theta \ \psi]^T \quad (1)$$

denotes the position and orientation, and

$$\boldsymbol{\nu} = [u \ v \ w \ p \ q \ r]^T \quad (2)$$

denotes linear and angular velocities. The position coordinates

$$\boldsymbol{p}^e = [x \ y \ z]^T \quad (3)$$

are decomposed in an Earth centered and Earth fixed frame (ECEF). However, for local navigation it is convenient to use

Table I
THE SNAME NOTATION FOR MARINE VESSELS

Motion components	Forces and moments	Linear and angular velocities	Position and Euler angles
surge (x -direction)	X	u	x
sway (y -direction)	Y	v	y
heave (z -direction)	Z	w	z
roll (rotation about x)	K	p	ϕ
pitch (rotation about y)	M	q	θ
yaw (rotation about z)	N	r	ψ

a local North East Down (NED) coordinate frame instead. Linear and angular velocities are decomposed in the body fixed frame.

The 6-DOF kinematic equations are written as

$$\dot{\boldsymbol{\eta}} = \boldsymbol{J}(\boldsymbol{\eta})\boldsymbol{\nu}, \quad (4)$$

where $\boldsymbol{J}(\boldsymbol{\eta})$ is a nonlinear transformation matrix.

IV. UNDERWATER VEHICLE DYNAMICS

The nonlinear dynamic equations of motion can be expressed in a compact form as [2]:

$$\dot{\boldsymbol{\eta}} = \boldsymbol{J}(\boldsymbol{\eta})\boldsymbol{\nu} \quad (5a)$$

$$\boldsymbol{M}\dot{\boldsymbol{\nu}} + \boldsymbol{C}(\boldsymbol{\nu})\boldsymbol{\nu} + \boldsymbol{D}(\boldsymbol{\nu})\boldsymbol{\nu} + \boldsymbol{g}(\boldsymbol{\eta}) = \boldsymbol{\tau} + \boldsymbol{w} \quad (5b)$$

where \boldsymbol{M} is the inertia matrix of the vehicle, $\boldsymbol{C}(\boldsymbol{\nu})$ is the centrifugal and coriolis matrix, $\boldsymbol{D}(\boldsymbol{\nu})$ is the hydrodynamic damping matrix and $\boldsymbol{g}(\boldsymbol{\eta})$ is the vector of gravity and buoyant forces, $\boldsymbol{\tau}$ is the control input vector of forces and moments, and \boldsymbol{w} is a vector of environment disturbances.

Equation (5) is not practical for controller or observer design. For slender and symmetric vehicles it is possible to separate the system into three noninteracting (or lightly interacting) systems [2], [6], [7]. The tree subsystems and their state variables are:

- Speed subsystem: $u(t)$
- Steering subsystem: $v(t), r(t), \psi$
- Diving subsystem: $w(t), q(t), \theta(t), z(t)$

The subsystems with states and control inputs for a cruciform tail configuration, are summarized in Table II. See also Fig. 2.

Table II
DECOUPLED SUBSYSTEMS OF AN UNDERWATER VEHICLE

Subsystem	State variables	Control inputs
Speed	$u(t)$	$n(t)$
Steering	$v(t), r(t), \psi$	$\delta_r(t)$
Diving	$w(t), q(t), \theta(t), z(t)$	$\delta_s(t)$

In the following, a simplified model for the horizontal dynamics will be described based on [6]. For a more detailed model of the HUGIN 4500 AUV see [8]. For general information about marine vehicle dynamics see for instance [2].

A. Speed subsystem

Neglecting interactions from other parts of the system, the surge subsystem can be modeled as

$$(m - X_{\dot{u}})\dot{u} - X_u u - X_{|u|u}|u|u = \tau_1(n) + T_{\text{loss}}, \quad (6)$$

where m is the mass of the vehicle, X_u is linear damping, $X_{|u|u}$ is quadratic damping, and T_{loss} contains coupling terms and environmental disturbances. For low speed applications $X_{|u|u} \approx 0$. The propeller dynamics can be modeled as

$$\tau_1 = T_{|n|n}|n|n + T_{un}|n|u \quad (7)$$

where $T_{|n|n}$ and $T_{un}|n|u$ are propeller coefficients and n is the propeller revolution.

B. Steering subsystem

Under the assumption of nearly constant speed $u \approx u_0$, the vehicle dynamics in sway and yaw can be simplified to:

$$m\dot{v} + mu_0 r = Y \quad (8)$$

$$I_z \dot{r} = N \quad (9)$$

where

$$Y = Y_{\dot{v}}\dot{v} + Y_{\dot{r}}\dot{r} + Y_v v + Y_r r + Y_{\delta}\delta_r \quad (10)$$

$$N = N_{\dot{v}}\dot{v} + N_{\dot{r}}\dot{r} + N_v v + N_r r + N_{\delta}\delta_r \quad (11)$$

For small roll and pitch angles we can assume that

$$\dot{\psi} \approx r. \quad (12)$$

The steering subsystem can then be rearranged as

$$\begin{bmatrix} m - Y_{\dot{v}} & Y_{\dot{r}} & 0 \\ -N_{\dot{v}} & I_z - N_{\dot{r}} & 0 \\ 0 & 0 & 1 \end{bmatrix} \begin{bmatrix} \dot{v} \\ \dot{r} \\ \dot{\psi} \end{bmatrix} + \begin{bmatrix} -Y_v & -Y_r + mu_0 & 0 \\ -N_v & -N_r & 0 \\ 0 & -1 & 0 \end{bmatrix} \begin{bmatrix} v \\ r \\ \psi \end{bmatrix} = \begin{bmatrix} Y_{\delta} \\ N_{\delta} \\ 0 \end{bmatrix} \delta_r \quad (13)$$

Writing the above equation in state space form yields

$$\begin{bmatrix} \dot{v} \\ \dot{r} \\ \dot{\psi} \end{bmatrix} = \begin{bmatrix} a_{11} & a_{12} & 0 \\ a_{21} & a_{22} & 0 \\ 0 & 1 & 0 \end{bmatrix} \begin{bmatrix} v \\ r \\ \psi \end{bmatrix} + \begin{bmatrix} b_1 \\ b_2 \\ 0 \end{bmatrix} \delta_r. \quad (14)$$

To calculate the horizontal position the kinematic differential equations are needed

$$\dot{n} = u \cos \psi - v \sin \psi \quad (15)$$

$$\dot{e} = u \sin \psi + v \cos \psi \quad (16)$$

C. Model discussion

The steering model (14) is in a convenient linear form. However, finding the coefficients a_{ij} and b_i is a nontrivial task. With accurate knowledge of the physical vehicle parameter, the coefficients can be calculated. Another approach is to estimate the coefficients directly based on measurements of v and r . This approach will be investigated in Section V. The downside of this approach is that the resulting model does not have a clear physical interpretation.

The AUV dynamics are inherently nonlinear. However, the linear models capture the most important dynamics and are accurate enough for applications like fault detection.

V. IDENTIFICATION PROCEDURE

Of the three almost decoupled sub-systems mentioned in Section IV, the steering dynamics is the most challenging one. Depth is measured quite accurately, and the engine runs with constant rpm most of the time, giving poor excitation of the speed dynamics. We will here describe how state-of-the-art algorithms are used to find a dynamic model that enables accurate simulation of steering dynamics. Simulation is in fact much more than what is required by sensor fusion algorithms for integrated navigation, fault diagnosis and control, where only the predictive ability of the model is important. The one-step or short-time prediction of a model is usually much more accurate than a batch simulation.

In summary, the system identification task is to estimate the parameters

$$\boldsymbol{\theta} = [a_{11} \ a_{12} \ a_{21} \ a_{22} \ b_1 \ b_2]^T \quad (17)$$

in the continuous-time physical model structure (14), given observations of $v(t)$, $r(t)$, $\delta_r(t)$ and the non-uniform sampling times t_k , $k = 1, 2, \dots, N$.

For the parameter identification, data collected during a sea-trial mission with the HUGIN 4500 vehicle were used. Prior to applying the identification procedure, the measurements were outlier filtered and smoothed using the navigation postprocessing tool NavLab [9]. This was done in order to enhance the accuracy.

The classical identification area concerns estimation of discrete time black box models from uniform sampled data [10]. We are here facing a grey-box identification problem, where there are still no standardized approaches [11], [12]. Our approach is as based on the non-linear least squares criteria

$$\hat{\boldsymbol{\theta}} = \arg \min_{\boldsymbol{\theta}} \sum_{k=1}^N (\mathbf{y}(t_k) - \hat{\mathbf{y}}(t_k; \boldsymbol{\theta}))^2 \quad (18)$$

where $\mathbf{y}(t_k) = [v(t_k) \ r(t_k)]^T$ is the measurement vector, and $\hat{\mathbf{y}}(t_k; \boldsymbol{\theta})$ is the simulation of the dynamic model (15) using the parameter vector $\boldsymbol{\theta}$.

The complete approach is as follows:

- 1) In order to get good initial values to the NLS optimization, a discrete time transfer function is first estimated.

Table III
ITERATIONS OF THE GAUSS-NEWTON ALGORITHM APPLIED TO (18)

Iteration	Cost	Gradient norm
0	$5.602 \cdot 10^2$	-
1	$5.531 \cdot 10^2$	$4.890 \cdot 10^3$
2	$5.525 \cdot 10^2$	$3.965 \cdot 10^3$

The single input multiple output (SIMO) model structure follows from (15) as

$$\begin{bmatrix} v(kT) \\ r(kT) \end{bmatrix} = G(z)\delta_r(kT). \quad (19)$$

This is identified using the following steps (see [10] for definitions and details):

- Resample the data regularly at a sampling frequency of 1Hz.
- Estimate a high order finite impulse response (FIR) model, where $G(z)$ has only zeros, no poles. This is done by the least squares method.
- Simulate noise-free measurements using the FIR model and true input.
- Estimate $G(z)$ as an ARX(2,2,1) model using the least squares method.

The ARX model could be estimated directly in step 1 above. The point with the second and third step is that so called output error model is obtained, which is much better suited for simulation than an ARX model. The resulting transfer function is

$$Y_1(z) = \frac{0.58 \cdot z - 0.31}{z^2 - 0.94 \cdot z + 0.027} U(z)$$

$$Y_2(z) = \frac{-11 \cdot z + 8.4}{z^2 - 0.94 \cdot z + 0.027} U(z)$$

- The discrete time transfer function is converted to a continuous time state space model with the structure (15) using the following steps:
 - Convert discrete time transfer function to discrete time state space model.
 - Apply inverse sampling to get a continuous time model.
 - Make a change of state variables to $\mathbf{x} := \mathbf{C}^{-1}\mathbf{x}$ so that the \mathbf{C} matrix becomes the identity matrix in the new coordinates

The resulting model is already on the form (15):

$$\dot{\mathbf{x}}(t) = \begin{bmatrix} 1.555 & 0.187 \\ -44.925 & -5.183 \end{bmatrix} \mathbf{x}(t) + \begin{bmatrix} 1.476 \\ -35.475 \end{bmatrix} u(t)$$

$$\mathbf{y}(t) = \begin{bmatrix} 1.000 & 0.000 \\ 0.000 & 1.000 \end{bmatrix} \mathbf{x}(t)$$

- NLS optimization.** The Gauss-Newton algorithm is applied to (18), using a continuous time ODE solver to produce the simulated $\hat{\mathbf{y}}(t_k)$ at non-uniformly sampled data. The ODE solver handles non-linear continuous time ODE's, though the model here is linear in the states.

The iterations of the Gauss-Newton algorithm are shown in Table III. In this case, the NLS cost (18) decreased only marginally, though the resulting model looks quite different from the initialization:

$$\dot{\mathbf{x}}(t) = \begin{bmatrix} 0.3 & 0.0 \\ -11.4 & -1.4 \end{bmatrix} \mathbf{x}(t) + \begin{bmatrix} 0.6 \\ -11.3 \end{bmatrix} u(t)$$

$$\mathbf{y}(t) = \begin{bmatrix} 1.0 & 0.0 \\ 0.0 & 1.0 \end{bmatrix} \mathbf{x}(t)$$

4) Validation by simulation.

Fig. 4 shows the simulation of the identified discrete time model, final continuous time model and measurements.

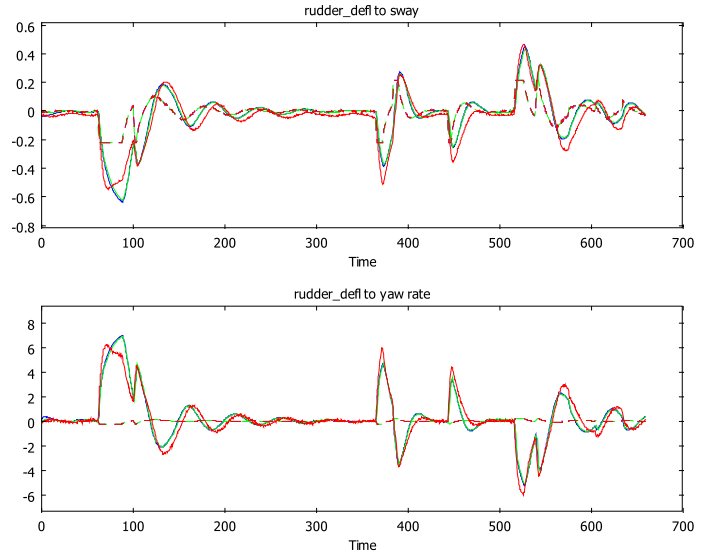


Figure 4. Simulation of identified discrete time model, final continuous time model and measurements.

- Cross validation.** A standard step in system identification to prevent overfitting observed data, is to validate the model on a new data set not used for estimation. An example with excellent performance is shown in Figure 4.

ACKNOWLEDGMENT

The authors are grateful to Kongsberg Maritime and the Norwegian Defence Research Establishment (FFI) for providing software and AUV data.

VI. TMP

[11], [13], [14]

REFERENCES

- R. Karlsson and F. Gustafsson, "Bayesian surface and underwater navigation," *IEEE Transactions on Signal Processing*, vol. 54, no. 11, pp. 4204–4213, Nov. 2006.
- T. I. Fossen, *Marine Control Systems. Guidance, Navigation, and Control of Ships, Rigs and Underwater Vehicles*. Trondheim, Norway: Marine Cybernetics, 2002.
- B. Jalving, "Depth accuracy in seabed mapping with underwater vehicles," in *OCEANS '99 MTS/IEEE. Riding the Crest into the 21st Century*, vol. 2, 1999, pp. 973–978 vol.2.

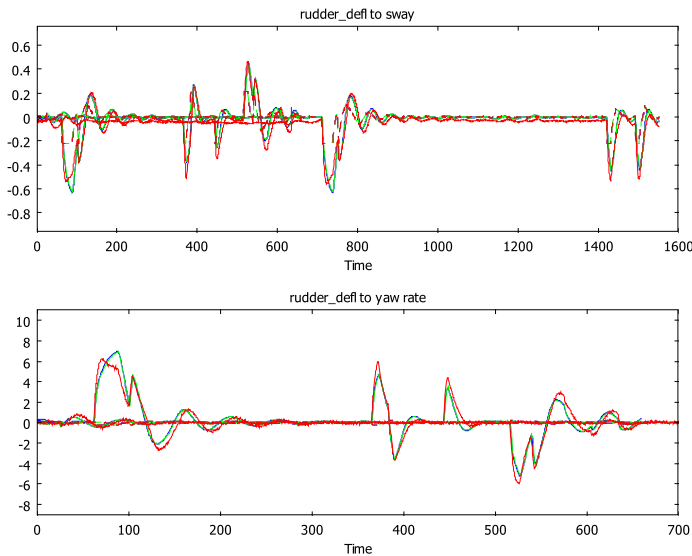


Figure 5. Same as Figure 4, but using cross validation on new data.

- [4] B. Jalving, K. Gade, O. K. Hagen, and K. Vestgard, "A toolbox of aiding techniques for the HUGIN AUV integrated inertial navigation system," *Modeling, Identification and Control*, vol. 25, no. 3, pp. 173–190, Jul. 2004.
- [5] SNAME, "The society of naval architects and marine engineers. nomenclature for treating the motion of a submerged body through a fluid," *Technical and Research Bulletin*, vol. 1–5, 1950.
- [6] B. Jalving, "The NDRE-AUV flight control system," *IEEE Journal of Oceanic Engineering*, vol. 19, no. 4, pp. 497–501, Oct. 1994.
- [7] L. Ni, "Fault-tolerant control of unmanned underwater vehicles," Ph.D. dissertation, Virginia Polytechnic Institute and State University, Department of Mechanical Engineering, 2001.
- [8] Øyvind Hegrenæs, O. Hallingstad, and B. Jalving, "Comparison of mathematical models for the HUGIN 4500 AUV based on experimental data," in *International Symposium on Underwater Technology (UT'07)*, Tokyo, Apr. 2007, (To appear).
- [9] K. Gade, "Navlab, a generic simulation and post-processing tool for navigation," *European Journal of Navigation*, vol. 2, no. 4, pp. 21–59, Nov. 2004.
- [10] L. Ljung, *System Identification – Theory For the User*, 2nd ed. Upper Saddle River, N.J.: Prentice Hall, 1999.
- [11] S. F. Graebe and T. Bohlin, "Identification of nonlinear stochastic grey box models: theory, implementation, and experiences," in *Selected Papers from the 4th IFAC Symposium on Adaptive Systems in Control and Signal Processing 1992.*, ser. IFAC Symposia Series, no. 8, Grenoble, France, 1993, pp. 47–52.
- [12] T. Bohlin, *Practical Grey-box Process Identification: Theory and Applications*. London: Springer-Verlag, 2006.
- [13] F. Tjarnstrom and L. Ljung, " L_2 model reduction and variance reduction," *Automatica*, vol. 38, no. 9, pp. 1517–1530, Sep. 2002.
- [14] P. Lindskog, "A system identification software tool for general miso arx-type of model structures," 1996. [Online]. Available: citeseer.ist.psu.edu/article/lindskog96system.html